Structural basis for anticodon recognition by discriminating glutamyl-tRNA synthetase

Shun-ichi Sekine[1,2], Osamu Nureki[1–3], Atsushi Shimada[2], Dmitry G. Vassylyev[2] and Shigeyuki Yokoyama[1–3]

[1]Cellular Signaling Laboratory, RIKEN Harima Institute at SPring-8, 1-1-1 Kouto, Mikazuki-cho, Sayo, Hyogo 679-5148, Japan. [2]Department of Biophysics and Biochemistry, Graduate School of Science, University of Tokyo, 7-3-1 Hongo, Bunkyo-ku, Tokyo 113-0033, Japan. [3]Genomic Sciences Center, RIKEN Yokohama Institute, 1-7-22 Suehiro-cho, Tsurumi, Yokohama 230-0045, Japan.

Glutamyl-tRNA synthetases (GluRSs) are divided into two distinct types, with regard to the presence or absence of glutaminyl-tRNA synthetase (GlnRS) in the genetic translation systems. In the original 19-synthetase systems lacking GlnRS, the 'non-discriminating' GluRS glutamylates both $tRNA^{Glu}$ and $tRNA^{Gln}$. In contrast, in the evolved 20-synthetase systems with GlnRS, the 'discriminating' GluRS aminoacylates only $tRNA^{Glu}$. Here we report the 2.4 Å resolution crystal structure of a 'discriminating' GluRS•$tRNA^{Glu}$ complex from *Thermus thermophilus*. The GluRS recognizes the $tRNA^{Glu}$ anticodon bases *via* two α-helical domains, maintaining the base stacking. We show that the discrimination between the Glu and Gln anticodons (^{34}YUC^{36} and ^{34}YUG^{36}, respectively) is achieved by a single arginine residue (Arg 358). The mutation of Arg 358 to Gln resulted in a GluRS that does not discriminate between the Glu and Gln anticodons. This change mimics the reverse course of GluRS evolution from anticodon 'non-dicsriminating' to 'discriminating'.

Aminoacyl-tRNA synthetase aminoacylates the cognate transfer RNA (tRNA) with the cognate amino acid, which will be incorporated into the nascent polypeptide chain on the ribosome. In addition to the attached amino acid, each aminoacyl tRNA has amino acid-specific nucleotide triplets (anticodons) that are complementary to the mRNA. Therefore, tRNAs act as 'adapter molecules' which link the genetic information with the protein sequence. Thus, accurate aminoacylation of tRNAs by these synthetases is important for the fidelity of translation.

Given the importance of accurate translation, each organism would be expected to have (at least) 20 aminoacyl-tRNA synthetases. However, in fact, most bacteria, archaea, chloroplasts, and mitochondria lack the aminoacyl-tRNA synthetase specific to glutamine (GlnRS)[1–4]. In these nineteen-synthetase systems, the aminoacyl-tRNA synthetase specific to glutamic acid (GluRS) aminoacylates both $tRNA^{Glu}$ and $tRNA^{Gln}$ with glutamic acid ('non-discriminating' GluRS), and the 'misacylated' product, Glu-$tRNA^{Gln}$, is converted to Gln-$tRNA^{Gln}$ by a transamidation enzyme. Interestingly, several taxons of bacteria have acquired a GlnRS, probably by horizontal gene transfer from the Eukaryota[5,6]. The twenty-synthetase systems changed their GluRS to be able to discriminate against $tRNA^{Gln}$ and, therefore, to specialize in $tRNA^{Glu}$ ('discriminating' GluRS)[7–9].

Phylogenetic analyses were not successful in identifying the amino acid residues specifically different between the non-discriminating and discriminating GluRSs, as the sequence conservation in the anticodon-binding domains is relatively low[6]. To elucidate the structural basis of tRNA recognition and discrimination by the 'discriminating' GluRS, we determined the crystal structure of the GluRS•$tRNA^{Glu}$ complex.

Overall structure

The crystal structure of the complex of the *T. thermophilus* GluRS[10] and $tRNA^{Glu}$ was solved and refined to a final R-factor of 21.9% (R-free = 29.8%) at 2.4 Å resolution (Fig. 1*a* and Table 1). In the crystals, one GluRS molecule binds one $tRNA^{Glu}$ molecule, and there are two enzyme•tRNA complexes (root mean square (r.m.s.) displacement = 0.90 Å over all the atoms) in the asymmetric unit. The overall structure of the tRNA-bound GluRS exhibits no significant differences from that of the tRNA-free enzyme[11], apart from some interdomain rotations (~7 °) and a local rearrangement in the vicinity of the active site. The GluRS interacts with the entire inner side of tRNA in an L-shaped structure (Fig. 1*a*), suggesting that the present structure is of an active complex.

Anticodon recognition

The anticodon loop of $tRNA^{Glu}$ exhibits the U-turn structure similar to that of yeast $tRNA^{Phe}$ (refs 12,13) (Fig. 1*a*,*b*). The minor groove side of the anticodon loop interacts with the GluRS C-terminal α-helical domains (4 and 5). These domains make a cavity large enough to accommodate all three of the anticodon nucleotides (C 34–U 35–C 36) stacked on each other. In contrast, the *Escherichia coli* GlnRS• $tRNA^{Gln}$ complex exhibits a substantial deformation of the anticodon loop[14,15]. The anticodon bases of $tRNA^{Gln}$ are not stacked on each other but trapped in different isolated pockets on GlnRS (Fig. 1*c*).

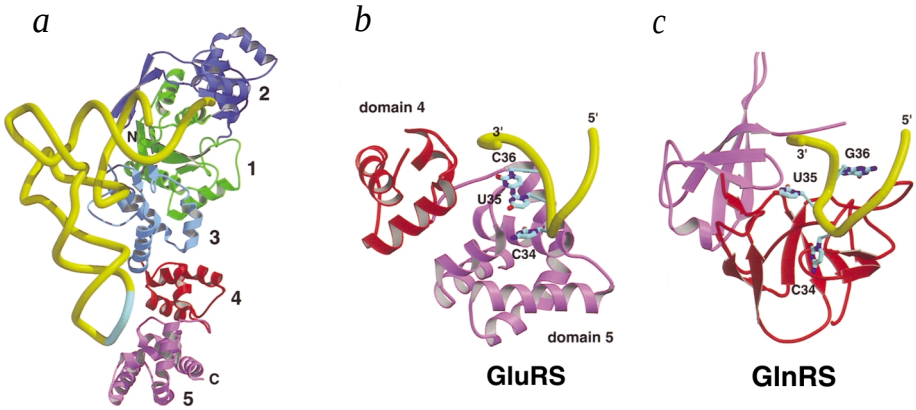

Fig. 1 Crystal structure of the complex. ***a***, Ribbon representation of the *T. thermophilus* GluRS•$tRNA^{Glu}$ complex structure. The Rossmann-fold (1), connective-peptide (2), stem-contact (3), and two anticodon-binding (4 and 5) domains[31] are green, deep blue, light blue, red, and purple, respectively. The tRNA molecule is highlighted in gold, except that the anticodon region is shown in cyan. ***b***, The anticodon bases within the $tRNA^{Glu}$ anticodon loop (the backbone is gold and the bases are cyan) and the GluRS domains 4 and 5. ***c***, The anticodon loop of $tRNA^{Gln}$ (the backbone is gold and the bases are cyan) in the GlnRS complex[15]. The figures were produced using the MOLSCRIPT[32] and RASTER3D[33] programs.

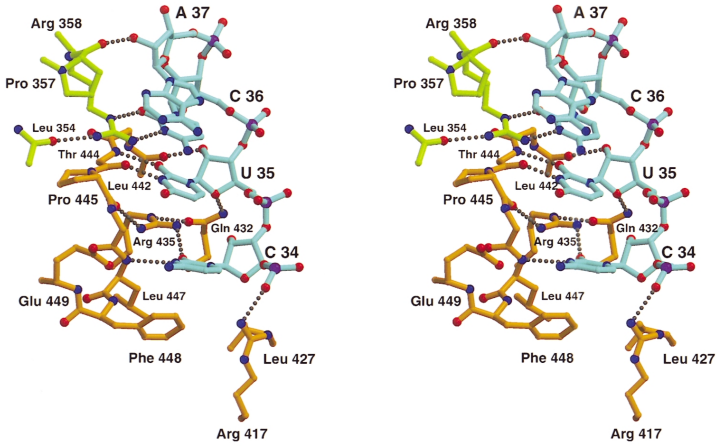

Fig. 2 The anticodon interface in the *T. thermophilus* GluRS•tRNA^{Glu} complex (stereo view). The anticodon-loop nucleotides, C 34, U 35, C 36, and A 37 are cyan. Amino acid residues of domains 4 and 5 are light green and orange, respectively.

The first and second nucleotides, C 34 and U 35, are recognized by an α-helix–loop–α-helix structure (residues 426–455) of domain 5 (Figs 1*b*, 2). The bottom side of C 34 interacts with the hydrophobic side chains of Leu 427, Leu 447, and Phe 448. The carbonyl group and the ring nitrogen at positions 2 and 3 of C 34 hydrogen bond with the side-chain guanidinium group of Arg 435 and the main chain amide group of Leu 447, respectively (Fig. 2). The Arg 435 side chain is fixed by hydrogen bonds with Gln 432 and Pro 445.

T. thermophilus GluRS can efficiently aminoacylate *E. coli* tRNA^{Glu} that has a modified uridine at position 34 (5-methylaminomethyl-2-thiouridine, mnm^{5}s^{2}U)[10]. In *E. coli*, this modification is indispensable for tRNA^{Glu} recognition by GluRS. The 2-thiocarbonyl and 4-carbonyl groups of mnm^{5}s^{2}U may hydrogen bond with the Arg 435 side chain and the Leu 427 main chain, respectively, while the 5-methylaminomethyl group can be accommodated in an open space. The C3′-*endo* ribose-ring puckering at position 34 is consistent with the proposal that the significant stabilization of the C3′-*endo* form by the 2-thiolation of U34 is important for the low K_m for *E. coli* tRNA^{Glu} (ref. 16). The U 35 base is recognized through the hydrogen bonds of the 2-carbonyl and 3-imino groups with the main-chain amide and carbonyl groups, respectively, of Thr 444 (Fig. 2). The ribose moiety of U 35 is held by the Gln 432 side chain and the Leu 442 main chain.

The third anticodon nucleotide (C 36) is specifically recognized by domain 4 (Figs 1*b*, 2). The carbonyl group and the ring nitrogen at positions 2 and 3 of C 36 hydrogen bond with the guanidinium group of a single Arg residue (Arg 358) (Figs 2, 3*a*). The Arg 358 side chain further hydrogen bonds with the Leu 354 main chain and is sandwiched between Pro 357 and the A 37 base on one side and Pro 445 on the other (Fig. 2). The Arg 358 residue is not well conserved all among the GluRSs, but is still completely conserved in the Proteobacteria β/γ subdivision and the *Thermus-Deinococcus* group[6], which employ the direct glutaminylation pathway[7–9] with 'discriminating' GluRS. The Leu 354 residue is also well conserved. On the other hand, among the C 34/U 35-recognizing residues described above, the only side chain involved in base-specific hydrogen bonding is that of Arg 435, and correspondingly, this Arg residue is completely conserved among all the GluRSs[6].

Discrimination between Glu and Gln anticodons

The identification of Arg 358 as the major determinant for the C 36 recognition provides the basis by which the *T. thermophilus* 'discriminating' GluRS[8] discriminates the Glu-type anticodon (^{34}YUC^{36}) from the Gln type (^{34}YUG^{36}) (Figs. 2, 3*a*). The protonated guanidinium group of Arg would cause steric hindrance with the bulky guanine base, and is unfavorable for recognition of the 1-imino and 2-amino groups (Fig. 3*b*). It is impossible for G 36 to achieve favorable interactions with Arg 358 by adopting the *syn* conformation since it would cause a serious and unavoidable steric hindrance between the 2-amino and 5′-phosphate groups of G 36 (not shown). Actually, we prepared a tRNA^{Glu} transcript with the mutation of C 36 to G. The C36G mutation considerably impaired the turnover number (k_{cat}) of GluRS, resulting in a more than 100-fold decrease in the k_{cat}/K_m relative to the wild type transcript (C 36) (Table 2).

A point mutation relaxes the anticodon specificity

The Gram-positive bacteria from the *Bacillus-Clostridium* group, which synthesizes Gln-tRNA^{Gln} through the transamidation pathway, have a conserved Gln at the position corresponding to Arg 358 of *T. thermophilus* GluRS (ref. 6). The smaller Gln side chain would not cause the steric clash with the bulky guanine base, and its polar side chain may allow recognition of both of cytosine and guanine (Fig. 3*c*,*d*). A *T. thermophilus* GluRS mutant with the replacement of Arg 358 by Gln (R358Q) was prepared, and its glutamylation efficiencies towards the wild type (C 36) and variant (C36G) tRNA^{Glu} transcripts were analyzed (Table 2). The R358Q mutant enzyme aminoacylates the two tRNA species with equal efficiency, and therefore is non-dis-

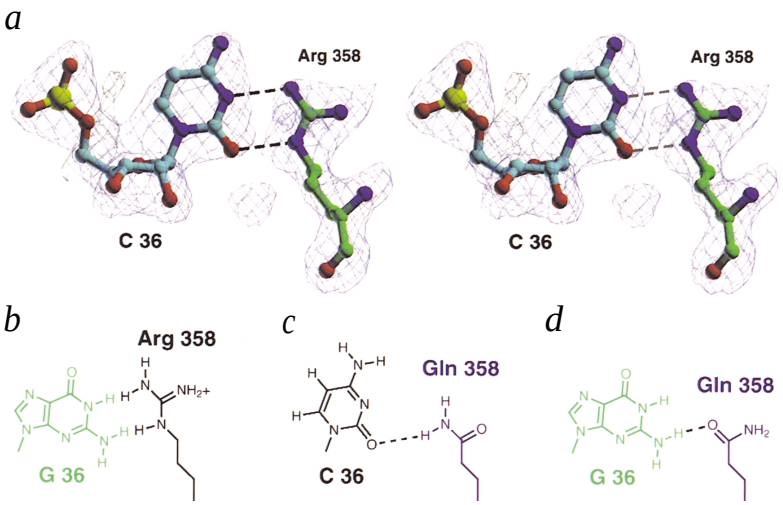

Fig. 3 The third anticodon base recognition. ***a***, A stereo view of the Arg 358–C 36 interactions in the crystal structure and the $|F_o-F_c|$ simulated-annealing omit electron density map (3 σ). ***b***, Modeling of the C 36→G 36 substitution (the Gln-type anticodon). ***c***, C 36 and ***d***, G 36 recognition by Gln 358, shown on the basis of modeling.

criminating with respect to the anticodon recognition. Although the K_m value of each tRNA substrate is larger than that of the wild type $tRNA^{Glu}$ for the wild type GluRS, the k_{cat} is comparable. The k_{cat}/K_m value of the present non-discriminating mutant GluRS is ~20 times lower than that of the wild type (Table 2), which is in agreement with the previous observation that the *Bacillus subtilis* non-discriminating GluRS exhibited similar low activity[1]. Thus, the single R358Q mutation, which was actually achieved through a single base change in the codon (CGG → CAG), transformed the discriminating *T. thermophilus* GluRS to an anticodon non-discriminating synthetase. We suggest that this particular Gln residue defines the dual anticodon specificity of the non-discriminating GluRSs of the Gram-positive bacteria. The reverse reaction, a Gln→Arg mutation in a non-discriminating GluRS, would switch the anticodon specificity to be discriminating.

Evolutionary implications

For the transition of the Gln-$tRNA^{Gln}$ synthesis route from the indirect transamidation pathway to the direct glutaminylation, the evolution of the tRNA specificity of GluRS is essential. The occurrence of GlnRS is phylogenetically scattered in the Bacteria[17]. The dispersed GlnRS distribution suggests that the evolution of the tRNA specificity of GluRS has occurred multiply in parallel after the division of the contemporary bacterial classes[17]. This parallel evolution might have been facilitated, if only a single base substitution in the gene was actually enough to change the specificity for the third anticodon base. Intriguingly, *Helicobacter pylori*, an ε proteobacterium, lacks GlnRS, but possesses two genes encoding GluRS[6,18]. In one *H. pylori* GluRS, the determinant Arg residue may specifically recognize C 36 in $tRNA^{Glu}$. In contrast, the other *H. pylori* GluRS has Glu, rather than Arg, in this position, which may prefer G 36 to C 36. This may represent an intermediate stage in evolution.

The anticodons of $tRNA^{Asp}$ and $tRNA^{Asn}$ also differ in only the third position. Some Archaea lack asparaginyl-tRNA synthetase, and employ a 'non-discriminating' aspartyl-tRNA synthetase (AspRS) for the transamidation pathway of Asn-$tRNA^{Asn}$ synthesis[19]. However, the evolutionary mechanism to change the anticodon specificity of the AspRSs seems to be fundamentally different from that of the GluRSs. The 'discriminating' AspRS recognizes the third anticodon nucleotide by a polypeptide loop through backbone interactions[20], whereas the 'non-discriminating' enzyme is likely to be insensitive to the third nucleotide, as the corresponding loop is much shorter[21].

It has been reported that engineered methionyl- and isoleucyl-tRNA synthetases, which are evolutionarily close to each other, exhibit an anticodon-specificity switch as a result of a single amino-acid substitution[22,23]. Further studies based on the synthetase-tRNA structures, like the present study, would promote understanding of the mechanisms of the evolutionary change in the anticodon specificity between the two closely related systems.

Table 1 Data collection and refinement statistics

Data set	
Space group	$C222_1$
Cell dimensions	a =109.98, b =218.67, c =134.67 Å
Resolution (Å)	50 – 2.4
Total reflections	251910
Unique reflections	56248
Completeness (%)	88.5 (74.0)[1]
R_{merge} (%)[2]	10.9 (34.0)[1]
Refinement statistics	
Resolution (Å)	30 – 2.4
Reflections	56215
R_{cryst} (%)[3]	21.9
R_{free} (%)[3]	29.8
Number of atoms	
Protein	7626
tRNA	3194
Water	272
R.m.s. deviations	
Bonds (Å)	0.013
Angles (°)	1.5
Improper angles (°)	0.71

[1]In the brackets, completeness and R_{merge} in the last resolution shell are listed, respectively.
[2]$R_{merge} = \Sigma_{hkl}\Sigma_j|I_j(hkl) - \langle I(hkl)\rangle|/\Sigma_{hkl}\Sigma_j|I_j(hkl)|$, where $I_j(hkl)$ and $\langle I(hkl)\rangle$ are the intensity of measurement j and the mean intensity for the reflection with indices hkl, respectively.
[3]$R_{cryst,\ free} = \Sigma_{hkl}||F_{calc}(hkl)| - |F_{obs}(hkl)||/\Sigma_{hkl}|F_{obs}|$, where the crystallographic R-factor is calculated including and excluding refinement reflections. The free reflections constituted 5 % of the total number of reflections.

Methods

Crystallization, data collection, and structure determination. *T. thermophilus* GluRS was expressed in *E. coli* JM109(DE3) and purified as described[11]. *T. thermophilus* $tRNA^{Glu}$ was prepared by *in vitro* transcription with T7 RNA polymerase as described[24,25]. Cocrystals were grown by the hanging drop vapor diffusion technique using 22% polyethylene glycol 1500, 37 mM Mops-Na (pH 6.7), 37 mM ammonium sulfate, 1% 2-methyl-2,4-pentandiol, 10 mM $MgCl_2$, and 5 mM 2-mercaptoethanol as the precipitant. Data were collected up to 2.4 Å resolution from the frozen crystals at 100 K using synchrotron radiation on BL6A at the Photon Factory (Tsukuba, Japan). They belong to the space group $C222_1$, with unit cell dimensions a = 109.98, b = 218.67, c = 134.67 Å. The data were processed with the programs DENZO and SCALEPACK[26] (Table 1).

The structure was solved by molecular replacement using the AMORE program[27] and the coordinates of the tRNA-free GluRS[11] as a search model. The manual model was built with the O program[28], and the refinement was carried out with the X-PLOR program[29]. The final R-factor was 21.9% (R-free = 29.8%) at 2.4 Å (Table 1). The final model has 88.3% of the residues in the most favorable region of the Ramachandran plot, as indicated by the program PROCHECK[30].

Table 2 Glutamylation kinetics of GluRSs

	GluRS (wild type)				GluRS (R358Q)			
	k_{cat} (s^{-1})	K_m (μM)	k_{cat}/K_m (relative)	$\Delta\Delta G^{\ddagger 1}$ (kcal/mol)	k_{cat} (s^{-1})	K_m (μM)	k_{cat}/K_m (relative)	$\Delta\Delta G^{\ddagger}$ (kcal/mol)
Substrates								
$tRNA^{Glu}$ (wild type)	2.1	4.7	1	0	1.5	85	0.039	2.2
$tRNA^{Glu}$ (C36G)	0.18	43	0.0095	3.1	1.4	55	0.057	1.9

[1]The change in the free energy of transition-state formation is given by the following. $\Delta\Delta G^{\ddagger} = -RT \ln \{(k_{cat}/K_m) / (k_{cat}/K_m)_{ref}\}$, where R is the gas constant, T is temperature, and $(k_{cat}/K_m)_{ref}$ is the k_{cat}/K_m value of wild type GluRS for wild type $tRNA^{Glu}$ transcript.

Preparation of the GluRS mutant and steady-state kinetics. The expression plasmid for the mutant GluRS (R358Q) was generated from the vector for the wild-type GluRS by changing a CGG (Arg) codon to CAG (Gln), using the PCR technique. The sequence of the gene was confirmed by DNA sequencing. The mutant GluRS was expressed in *E. coli* cells, and was purified according to the procedure used for the wild type enzyme. The heat treatment (70 °C for 1 h) before the column chromatography efficiently eliminates the

wild-type GluRS in the host *E. coli* cells[10,11]. *E. coli* $tRNA^{Glu}$ transcripts (wild type and C36G)[24] were used for examinations of the GluRS activities. Aminoacylation reactions were carried out as described previously[24,25], at 65 °C. The typical ratio of the tRNA and enzyme concentrations was more than 50:1. Kinetic parameters were obtained by Lineweaver-Burk plots (Table 2).

Coordinates. The coordinates have been deposited in the Protein Data Bank (accession code 1G59).

Acknowledgments
S.Y. is the recipient of Grants-in-Aid for Science Research on Priority Areas from the Ministry of Education, Science, Sports and Culture of Japan; S.S. was supported by grants from the JSPS Research Fellowships for Young Scientists and from the RIKEN Special Postdoctoral Researchers Program.

Correspondence should be addressed to D.G.V. *email: dmitry@yumiyoshi.harima.riken.go.jp* and S.Y. *email: yokoyama@biochem.s.u-tokyo.ac.jp*

Received 20 September, 2000; accepted 19 December, 2000.

1. Lapointe, J., Duplain, L. & Proulx, M. *J. Bacteriol.* **165**, 88–93 (1986).
2. Schön, A., Kannangara, G., Gough, S. & Söll, D. *Nature* **331**, 187–190 (1988).
3. Rogers, K.C. & Söll, D. *J. Mol. Evol.* **40**, 476–481 (1995).
4. Gagnon, Y., Lacoste, L., Champagne, N. & Lapointe, J. *J. Biol.Chem.* **271**, 14856–14863 (1996).
5. Lamour, V. *et al. Proc. Natl. Acad. Sci. U. S. A.* **91**, 8670–8674 (1994).
6. Siatecka, M., Rozek, M., Barciszewski, J. & Mirande, M. *Eur. J. Biochem.* **256**, 80–87 (1998).
7. Curnow, A.W., Tumbula, D.L., Pelaschier, J.T., Min, B. & Söll, D. *Proc. Natl. Acad. Sci. U. S. A.* **95**, 12838–12843 (1998).
8. Becker, H.D. & Kern, D. *Proc. Natl. Acad. Sci. U. S. A.* **95**, 12832–12837 (1998).
9. Handy, J. & Doolittle, R.F. *J. Mol. Evol.* **49**, 709–715 (1999).
10. Hara-Yokoyama, M., Yokoyama, S. & Miyazawa, T. *J. Biochem.* **96**, 1599–1607 (1984).
11. Nureki, O. *et al. Science* **267**, 1958–1965 (1995).
12. Robertus, J.D. *et al. Nature* **250**, 546–551 (1974).
13. Kim, S.H. *et al. Science* **185**, 435–440 (1974).
14. Rould, M.A., Perona, J.J., Söll, D. & Steitz, T.A. *Science* **246**, 1135–1142 (1989).
15. Rould, M.A., Perona, J.J. & Steitz, T.A. *Nature* **352**, 213–218 (1991).
16. Madore, E., *et al. Eur. J. Biochem.* **266**, 1128–1135 (1999).
17. Brown, J.R. & Doolittle, W.F. *J. Mol. Evol.* **49**, 485–495 (1999).
18. Tomb, J.F. *et al. Nature* **388**, 539–547 (1997).
19. Curnow, A.W., Ibba, M. & Söll, D. *Nature* **382**, 589–590 (1996).
20. Cavarelli, J., Rees, B., Ruff, M., Thierry, J.-C. & Moras, D. *Nature* **362**, 181–184 (1993).
21. Schmitt, E. *et al. EMBO J.* **17**, 5227–5237 (1998).
22. Auld, D.S. & Schimmel, P. *Science* **267**, 1994–1996 (1995).
23. Auld, D.S. & Schimmel, P. *EMBO J.* **15**, 1142–1148 (1996).
24. Sekine, S. *et al. J. Mol. Biol.* **256**, 685–700 (1996).
25. Sekine, S., Nureki, O., Tateno, M. & Yokoyama, S. *Eur. J. Biochem.* **261**, 354–360 (1999).
26. Otwinowski, Z. & Minor, W. In *Methods Enzymol.*, Vol. 276. (eds. Carter, C.W.J. & Sweet, R.M.) 307–325 (Academic Press, London; 1997).
27. CCP4 *Acta Cryst.* **D50**, 760–763 (1994).
28. Jones, T.A., Zou, J.-Y., Cowan, S.W. & Kjeldgaard, M. *Acta Cryst.* **A47**, 110–119 (1991).
29. Brünger, A.T. *X-PLOR: a system for X-ray crystallography and NMR.* (Yale Univ. Press, New Haven; 1992).
30. Laskowski, R.A., MacArthur, M.W., Moss, D.S. & Thornton, J.M. *J. Appl. Cryst.* **26**, 283–291 (1993).
31. Sugiura, I. *et al. Structure Fold. Des.* **8**, 197–208 (2000).
32. Kraulis, P.J. *J. Appl. Cryst.* **24**, 946–950 (1991).
33. Merritt, E.A. & Murphy, M.E.P. *Acta Cryst.* **D50**, 869–873 (1994).

Structure of the RTP–DNA complex and the mechanism of polar replication fork arrest

J.A. Wilce[1], J.P.Vivian[2], A.F. Hastings[3], G. Otting[4], R.H.A. Folmer[5], I.G. Duggin[3], R.G. Wake[3] and M.C.J. Wilce[2]

[1]Department of Chemistry/Biochemistry University of Western Australia and the Western Australian Institute for Medical Research, Nedlands, Western Australia 6907, Australia. [2]Department of Pharmacology/Crystallography Centre, University of Western Australia, and the Western Australian Institute for Medical Research, Nedlands, Western Australia 6907, Australia. [3]Department of Biochemistry, University of Sydney, Sydney, New South Wales 2006, Australia. [4]Department of Medical Biochemistry and Biophysics, Karolinska Institute, S-171 77 Stockholm, Sweden. [5]Structural Chemistry Laboratory, AstraZeneca R&D, S-431 83 Mölndal, Sweden.

The coordinated termination of DNA replication is an important step in the life cycle of bacteria with circular chromosomes, but has only been defined at a molecular level in two systems to date. Here we report the structure of an engineered replication terminator protein (RTP) of *Bacillus subtilis* in complex with a 21 base pair DNA by X-ray crystallography at 2.5 Å resolution. We also use NMR spectroscopic titration techniques. This work reveals a novel DNA interaction involving a dimeric 'winged helix' domain protein that differs from predictions. While the two recognition helices of RTP are in close contact with the B-form DNA major grooves, the 'wings' and N-termini of RTP do not form intimate contacts with the DNA. This structure provides insight into the molecular basis of polar replication fork arrest based on a model of cooperative binding and differential binding affinities of RTP to the two adjacent binding sites in the complete terminator.

The replication terminator protein (RTP) of *Bacillus subtilis* is one of only two well-characterized proteins known to cause DNA replication fork arrest[1–3]. It is a 29 kDa dimeric member of the 'winged helix' family of DNA binding proteins[4] that shows exceptionally high affinity for its cognate DNA binding sites (K_d ~10^{-11} M^{-1}) and an even higher affinity for them when in the functional terminator complex, which includes two adjacently bound RTP dimers[5]. DNA replication in *Bacillus subtillis* involves the bidirectional replication of the circular chromosome from a specific replication 'origin'[2]. Clockwise and anticlockwise replication forks meet and fuse in a restricted 'terminus' region located approximately opposite the origin. This is mediated by 30 base pair (bp) DNA sequences (*Ter* sites) to which RTP molecules bind and thus impede the progress of the replicative machinery. The *Ter* sites are organized into two opposed groups that are polar in action; one set is designed to block the anticlockwise replication fork, while the other set blocks the clockwise replication fork. Thus, the two sets of opposed *Ter* sites act in concert as a replication fork trap[6]. An analogous system has been characterized in *Escherichia coli*; however, neither the *Ter* site DNA nor the replication terminator proteins from *B. subtilis* and *E. coli* bear any sequence or structural homology[1,3,5,7].

The primary structures of the *Ter* sequences within several species of *B. subtilis* have been characterized, and the consensus motif effecting polar fork arrest is well defined[8]. Each 30 bp *Ter* sequence in *B. subtilis* contains two pseudosymmetric and overlapping binding sites for RTP dimers, a high affinity B site and a relatively low affinity A site. RTP binds cooperatively to the A site once the B site is filled[5,9]. The replication fork is blocked when it approaches the *Ter* site from the B direction. When it approaches from the other direction, however, it is able to pass unimpeded through the terminator.

Although the structure of apo-RTP has been reported[4], the structural basis of polar replication fork arrest is not yet under-